Integrative analysis of the transcriptome and targetome identifies the regulatory network of miR-16: An inhibitory role against the activation of hepatic stellate cells[1]

Qin Pan[1], Canjie Guo[2], Chao Sun[1], Jiangao Fan[1,3,*] and Chunhua Fang[4,*]

[1]*Department of Gastroenterology, Xinhua Hospital, School of Medicine, Shanghai Jiao Tong University 200092, 1665 Kong Jiang Rd., Shanghai, China*
[2]*Digestive Disease Laboratory and Department of Gastroenterology, Ren Ji Hospital, School of Medicine, Shanghai Jiao Tong University 200001, 2000 Jiang Yue Rd., Shanghai, China*
[3]*Shanghai Key Laboratory of Children's Digestion and Nutrition 200092, 1665 Kong Jiang Rd., Shanghai, China*
[4]*School of Electronics and Information Engineering, Tong Ji University, 201804, 4800 Cao An Rd., Shanghai, China*

Abstract. Hepatic stellate cell (HSC) activation is the critical event of liver fibrosis. Abnormality of miR-16 expression induces their activation. However, the action model of miR-16 remains to be elucidated because of its multiple-targeted manner. Here, we report that miR-16 restoration exerted a wide-range impact on transcriptome (2,082 differentially expressed transcripts) of activated HSCs. Integrative analysis of both targetome (1,195 targets) and transcriptome uncovered the miR-16 regulatory network based upon bio-molecular interaction databases (BIND, BioGrid, Tranfac, and KEGG), cross database searching with iterative algorithm, Dijkstra's algorithm with greedy method, *etc*. Eight targets in the targetome (*Map2k1, Bmpr1b, Nf1, Pik3r3, Ppp2r1a, Prkca, Smad2,* and *Sos2*) served as key regulatory network nodes that mediate miR-16 action. A set of TFs (*Sp1, Jun, Crebl, Arnt, Fos,* and *Nf1*) was recognized to be the functional layer of key nodes, which mapped the signal of miR-16 to transcriptome. In result, the comprehensive action of miR-16 abrogated transcriptomic characteristics that determined the phenotypes of activated HSCs, including active proliferation, ECM deposition, and apoptosis resistance. Therefore, a multi-layer regulatory network based upon the integration of targetome and transcriptome may underlie the global action of miR-16, which suggesting it plays an inhibitory role in HSC activation.

Key words: miR-16, hepatic stellate cell, targetome, transcriptome, network

---

[1]Qin Pan and Canjie Guo contributed equally to this work.

*Corresponding authors: Jiangao Fan, Department of Gastroenterology, Xinhua Hospital, School of Medicine, Shanghai Jiao Tong University 200092, 1665 Kong Jiang Rd., Shanghai, China. Tel. 86-021-65790000; Fax: 86-021-25078999; E-mail: fanjiangao@gmail.com.
    Chunhua Fang, School of Electronics and Information Engineering, Tong Ji University, 201804, 4800 Cao An Rd., Shanghai, China. Tel.: 86-021-52842095; Fax: 86-021-69589979; E-mail: chunhua_fang@163.com.

1. Introduction

Hepatic stellate cells (HSCs) are mesenchymal cells with vitamin A-containing lipid droplets in the liver. Upon stimulation, they experience phenotypic transdifferentiation, also known as activation, toward myofibroblast. Activated HSCs serve as effector cells in the initiation as well as the progression of liver fibrogenesis [1]. Thus, activated HSCs qualify them to be a therapeutic target of liver fibrosis/cirrhosis.

Presently, miR-16 is proved to be a critical regulator in HSCs. miR-16 administration significantly reduces Bcl-2 expression, which is responsible for the apoptosis resistance of activated HSCs. This elevates apoptosis rate by activation of caspases [1]. Moreover, restoring intracellular miR-16 inhibits the translational level of cyclinD1 (CCND1), a pivotal member of the cell cycle. Thus, activated HSC proliferation is restricted as a result of cell-cycle arrest [1]. However, despite its potential role in diminishing activated HSCs, miR-16 is still not incorporated into fibrosis prevention because of its multiple targets and, subsequently, the indefiniteness of its global action.

Fortunately, recent studies uncovered that a single miRNA is able to comprehensively shift the cellular transcriptome towards another status in which it is specially expressed [2]. Furthermore, signal transduction from the miRNA-specific targetome to the transcriptome has been suggested to underlie the global action of miRNA. We, therefore, obtained the targetome of miR-16 by the miRanda and TargetScan databases. miR-16's effect on the transcriptome of activated HSCs was investigated by miR-16 restoration and array hybridization. Then, a multiple-layer regulatory network, which mediates the signal transduction from the targetome to the transcriptome, was constructed based upon biomolecular interaction databases, cross database searching with iterative algorithm, Dijkstra's algorithm with greedy method, *etc*. Consequently, the global role of miR-16 in HSC activation was highlighted by integrating the targetome, transcriptome, and miR-16 regulatory network.

2. Materials and methods

2.1. miR-16 treatment of HSCs

Activated HSCs were isolated from adult male Sprague-Dawley rats (Shanghai Laboratory Animal Center of the Chinese Academy of Sciences), that had carbon tetrachloride (CCl_4)-induced liver fibrosis, by *in situ* perfusion and density-gradient centrifugation. HSCs purity was 90% when assessed by the significant expression of a-SMA and desmin, and negative expression of albumin (ALB), CD31, CD68, and cytokeratin-19 (CK-19) [1]. All procedures conformed to guidelines laid out by the World Medical Assembly (Declaration of Helsinki) and were approved by the Ethical Committee of Xinhua Hospital.

Recombinant Lentiviruses (pLV-miR-16 and pLV-GFP) were constructed by the co-transfection of miRNA expression vectors [either with precursor rno-miR-16 (pre-rno-miR-16, MI0000844) (pCDH-CMV-MCS-EF1-copGFP-miR-16) or without rno-miR-16 exogenous oligonucleotides (pCDH-CMV-MCS-EF1-copGFP)] and the Lentivirus Package plasmid mix (System Biosciences, Mountain View, CA, U.S.A.) in 293TN cells as previously described [1].

Exponentially growing activated HSCs were then divided into pLV-miR-16-treated and pLV-GFP-treated groups at random and then infected with pLV-miR-16 and pLV-GFP, respectively, at 1.0×10^8 transduction units (TU)/ml. As detected by stem–loop RT and real-time PCR [1], the miR-16 level in

the pLV-miR-16-treated group elevated approximately 2-fold. However, the miR-16 expression remained constant in the pLV-GFP-treated group.

2.2. Microarray hybridization for the miR-16-regulated transcriptome

The total RNA of the HSCs, derived from both the pLV-miR-16-treated group (n=3) and the pLV-GFP-treated group (n=3) 48 h after the lentivirus transfection, was extracted using the TRIzol reagent. After RNA purification and cRNA preparation, Affymetrix rat 230 2.0 arrays (Affymetrix, Santa Clara, U.S.A.) were hybridized with biotin-labeled RNA probes.

Random variance model (RVM) was employed to normalize the obtained data, and to filter the significantly up-regulated and down-regulated transcripts on the basis of P value of RVM t-test (<0.05) and false discovery rate (FDR) (<0.05) [3]. RT-QPCR for 6 randomly selected genes, *Cav1*, *ICAM1*, *Mmp2*, *Ezr*, *Casp3* and *Col1a1*, confirmed the reliability of the array hybridization.

2.3. Targetome analysis of miR-16

Taking advantage of the widely accepted arithmetics covering *Rattus Norvegicus*, the miR-16 targets were obtained by the following databases: miRBase [4] and TargetScan [5], respectively. These predicted targets of were pooled to construct the targetome of miR-16.

2.4. Bioinformatics modeling for the regulatory network of miR-16 in HSCs

To purse the signal transduction from miR-16 targets to miR-16-regulated transcripts, the miR-16 targetome was designed to be a set of upstream proteins. Downstream proteins of the miR-16 targets were then found by multiple-step, trans-database iterative search, including BIND [6], BioGrid [7] and KEGG [8], on the basis of protein-protein interactions. On the other side, we use Tranfac database [9] to enquire the transcription factors (TFs) up-stream to miR-16-regulated transcripts on the basis of TF-mRNA binding. In result, a set of TFs were identified to be both the downstream protein of miR-16 targets and the up-stream protein of miR-16-regulated transcripts. Thus a regulatory network, connecting miR-16 targets, TFs, and miR-16-regulated transcripts, was generated.

Thereafter, we assigned the miR-16 targets and target-related TFs to be source vertex and target vertex, respectively. Dijkstra's algorithm with greedy method was performed to uncover the shortest path from source vertex to target vertex (Figure 1). Depending on this optimization, the HSC-specific regulatory network of miR-16 with fewest node numbers was resultantly constructed. Moreover, we scored the Degree of each node, which reflected the sum of interactions between one node and the others, so as to evaluate the crucial ones in the network [10].

According to the annotation of KEGG database, sub-networks relating to signal pathways were recognized and validated by normalized enrichment scoring (NES), Fisher's exact test and FDR analysis [11]. Those signal-pathway-based sub-networks with *P*-value less than 0.05 and FDR less than 0.05 were defined to be statistical significance.

2.5. Statistical analysis

The fold change of gene expression is expressed as mean ± standard deviation (SD). The statistical analysis was done with Student's t-test for comparing two groups. Differences with $P < 0.05$ were considered statistically significant.
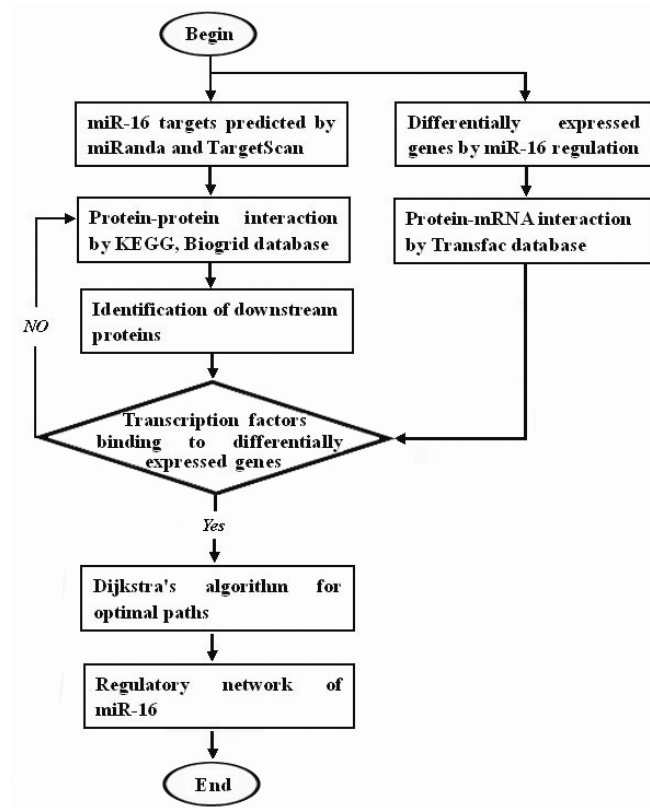
Fig. 1. Flow chart for the construction of miR-16 regulatory network.

3. Results

3.1. Effect of miR-16 on the transcriptome of HSCs

In contrast to the pLV-GFP-treated HSCs, 1,162 transcripts (representing 3.74% of the total) were determined to be significantly up-regulated in the pLV-miR-16-treated HSCs at 48 hours. Meanwhile, 920 transcripts (2.96%) were statistically lowered under miR-16 control.

Most notably, miR-16-induced transcriptional characteristics strongly hindered HSC activation, as demonstrated by the following conclusions: (1) Genes that are critical for HSC proliferation, such as *Cdc2*0, *Pttg1*, and *Wee1*, were expressed at decreased levels. Negative cell cycle regulators (*e.g.*, *Cdkn1a*) were expressed at a level that was 6.63-fold above normal (Table 1). (2) Differentially expressed genes that are specific for ECM synthesis, secretion and degradation detailed the remaining action of miR-16 on the transcriptome. In detail, important fibrosis-inducing cytokines [*Tgfb2* and collagens (*Col1a1*, *Col3a1*, *Col5a3*, *Col12a1*)] exhibited significantly decreased expression, whereas the fibrolysis-dependent matrix metallopeptidases (*Mmp2*, *Mmp12*, *etc.*) had up-regulated transcription after the miR-16 treatment (Table 1). (3) Another noticeable phenomenon involved the genes that dominate mitochondrial apoptosis. Transcription of those that mediate the mitochondria-based apoptosis (including *Casp3*, *Casp9*, *Ddit3*, *Dffa*, *etc.*) increased 1.75-, 4.85-, 4.45-, and 1.59-fold within pLV-miR-16-treated HSCs (Table 1).

Table 1

Transcription factors mediate global effect of miR-16 on transcriptome

Gene	Accession No.	Fold Change	TF	Function
Cdc20	NM_171993	-1.63±0.56	Sp1	Proliferation
Cdkn1a	NM_080782	6.63±0.99	Sp1,Fos	Proliferation
Pttg1	NM_022391	-2.05±0.29	Sp1	Proliferation
Wee1	NM_001012742	-1.77±0.44	Sp1, Fos	Proliferation
Col1a1	NM_053304	-2.72±0.23	Sp1, Nf1	ECM metabolism
Col3a1	NM_032085	-14.83±3.22	Jun	ECM metabolism
Col5a3	NM_021760	-2.44±0.35	Sp1, Fos	ECM metabolism
Col12a1	XM_00106068	-2.33±0.13	Sp1, Fos	ECM metabolism
Mmp2	NM_03105	3.82±1.30	Jun, Fos	ECM metabolism
Mmp12	NM_053963	9.18±1.75	Crebl	ECM metabolism
P4ha3	XM_001066817	-2.53±0.61	Arnt	ECM metabolism
Tgfb2	NM_031131	-2.54±0.34	Crebl	ECM metabolism
Birc3	NM_023987	2.41±0.18	Sp1	Apoptosis
Casp3	NM_012922	1.75±0.43	Sp1	Apoptosis
Casp9	NM_031632	4.85±0.89	Arnt	Apoptosis
Ddit3	NM_024134	4.45±0.53	Jun	Apoptosis
Dffa	NM_053679	1.59±0.15	Sp1	Apoptosis
Serpine1	NM_012620	4.29±0.94	Sp1, Fos	Apoptosis

3.2. Prediction algorithm recognized the targetome of miR-16

By first evaluating the complementarity between the seed sequence of miRNA and the 3' untranslated region (3'UTR) of mRNA, 1,034 genes were predicted by the miRanda algorithm to be the miR-16 target. However, the TargetScan algorithm predicted a set of miR-16 targets that consisted of 182 genes. In result, a union set of 1,195 genes reflected the miR-16 targetome. This covered most of the experimentally proven target of miR-16, including cyclin D1 (*CCND1*), *Bcl-2*, and *Wnt3a*, *etc*.

3.3. Modeling of regulatory network identified the effect of miR-16 on HSC activation

Integrating the targetome, transcriptome, and bio-molecular interaction database outlined the regulatory network of miR-16 in activated HSCs (Figure 2). A group of miR-16 targets (*Map2k1*, *Bmpr1b*, *Nf1*, *Pik3r3*, *Ppp2r1a*, *Prkca*, *Smad2*, and *Sos2*) was suggested to be the central targetome components. They mediated the effect of miR-16 through various kinds of protein-protein interactions, being activation, indirect action, phosphorylation, inhibition, compound action on substrate, binding/association, and expression enhancing. Next, a set of TFs, including *Sp1, Jun, Crebl, Arnt, Fos*, and *Nf1*, served as the bottom layer of key nodes that are essential for the regulatory network (Figure 2). Differentially expressed genes, *i.e. Cdc20, Cdkn1a, Col1a1, Col3a1, Col5a3, Col12a1, Mmp2, Mmp12, Tgfb2, Casp3, Casp9, Ddit3,* and *Dffa*, were under the TF set's control (Table 1). A large majority of these genes determined the HSC phenotypes of proliferation, ECM metabolism and apoptosis.

Some sub-networks had been recognized on the basis of signal pathway, being TGFβ/Smad, PI3K/Akt, MAPK/ERK, and GnRH. Members of signal pathways (*i.e. Mapks, Hras*, *Nr*as, *Smads*, *Gsk3b*) and TFs (*i.e. Fos*, *Jun*) took the critical place of sub-networks because of their high-ranking score of Degree (Table 2).

4. Discussion

The unique pattern of miRNAs' function, which directly targets hundreds of genes, has been well described. Furthermore, target prediction is a powerful methodfor obtaining an overview of their targetome. According to the miRBase and TargetScan algorithms, the miR-16 targets were predicted to be 1, 034 and 182, respectively. However, some differences exist between the miRBase and TargetScan algorithms due to following reasons: inconsistency in target recognition, ranking of prediction
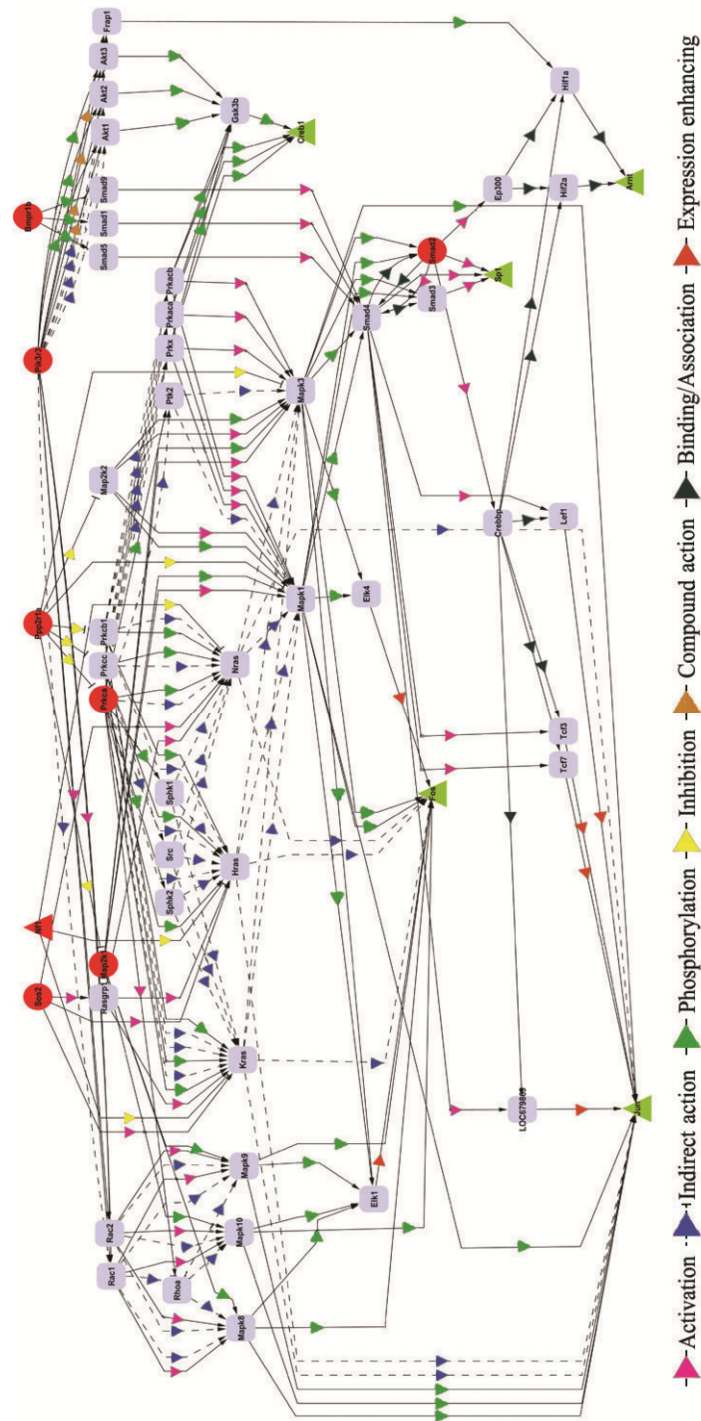
Fig. 2. Regulatory network of miR-16 in activated HSCs. Red circles, triangle represents predicted-targets and predicted-target TF, respectively. Green triangles represent TFs which bind to differentially expressed genes. Arrows labeled by rose, violet, green, yellow, ocher, navy and brown represent protein-protein interactions of activation, indirect action, phosphorylation, inhibition, compound action on substrate, binding/association, and expression enhancing, respectively.

efficacy, site conservation, *etc*. Therefore, to overcome the algorithm-based bias in target prediction, we pooled two sets of predicted targets to construct the miR-16 targetome.

Apart from its targetome, transcriptome analysis represents another important method for shedding light on the global action of miR-16. Indeed, array hybridization revealed the transcriptome-scale regulation of miR-16 after its restoration in the activated HSCs, which included 2,082 differentially expressed transcripts. Surprisingly, several characteristics were associated with the miR-16-induced tran

Table 2

Signal pathways serve as sub-networks of miR-16 regulatory network

Signal pathway	NES	*P* value	FDR
TGF-beta signaling pathway	4.291	0.004	0.015
Apoptosis	3.045	0.011	0.026
Cell cycle	2.450	0.020	0.029
PI3K-Akt signaling pathway	2.090	0.025	0.030
p53 signaling pathway	1.987	0.027	0.043
GnRH signaling pathway	1.814	0.031	0.045
MAPK signaling pathway	1.702	0.042	0.038
Ubiquitin mediated proteolysis	1.439	0.045	0.049

scriptome. Firstly, miR-16 facilitated the significant down-regulation of genes (*i.e. Cdc2*0, *Pttg1*, and *Wee1*) that are necessary for cell cycle and proliferation, whereas the strong up-regulation of genes (*i.e. Cdkn1a*) antagonizes these processes [12]. Secondly, miR-16 ameliorated the expression of the profibrogenic enzyme (*i.e. P4ha3*), cytokines (*i.e Tgfb2*) and collagens (*i.e. Col1a1, Col3a1, Col5a3, Col12a1*) as well as promoted ECM enzymolysis by MMPs (*i.e. Mmp2, Mmp1*) transcription [13]. Thirdly, miR-16 management introduced the high-level mRNAs (*i.e. Casp3, Casp9, Ddit3*, and *Dffa*) that are specific to mitochondrial apoptosis [14]. Therefore, the comprehensive effect of miR-16 abrogates the characteristic transcriptiome that determines pivotal phenotypes of activated HSCs, primarily the active proliferation, ECM deposition, and apoptosis resistance.

An action model of miR-16 was then established to integrate the targetome and transcriptome findings. It was focused on the signal flow from the miR-16 targets to the miR-16-regulated genes based upon protein-protein interaction and TF-mRNA binding, both of which were subjected to a cross-database iterative search of a major repository of protein and TF information. Thus, a complicated network consisting of numerous miR-16 targets, downstream proteins, and TFs was presented as the underlying foundation of the global action of miR-16. In order to highlight the crucial members, this regulatory network was optimized by exploring the single source shortest path. As a result, there were 55 nodes in the regulatory network, consisting of 8 (14.55%) miR-16 targets, 43 (76.36%) downstream proteins, and 6 (10.91%) TFs.

As defined by the signal flow in the regulatory network, the set of miR-16 targets was recognized to be the top layer of key nodes. They mediated the regulatory information of miR-16 through interacting with multiple down-steam proteins, which are usually signaling pathways members. In detail, the miR-16-induced inhibition of *Sos2* suppressed the MAPK/ERK signaling pathway *via* the inactivation of *Kras, Hras*, *Nras*, and *Rasgrp1* [15]. The expression loss of *Map2k1*, the other miR-16 target in the MAPK/ERK signaling pathway, also blocked the signal pathway *via* the inactivation of *Mapk1* and *Mapk3* as well as the dephosphorylation of *Mapk1, Mapk3, Mapk8, Mapk9*, and *Mapk10* [16]. Nevertheless, the targeted effect of miR-16 on *Bmpr1b* repressed the TGFβ/Smad signaling pathway by dephosphorylated *Smad1, Smad5*, and *Smad9* [17]. The complementarity between miR-16 and *Smad2* similarly impacted the TGFβ/Smad signaling through inactivation of *Smad4, Crebbp, Ep300*, and *Sp1*

as well as less binding/association of *Smad4* [18]. Another important target of miR-16, *Pik3r3*, was demonstrated to activate *Rac1* and *Rac2*, whereas it affected *Akt1, Akt2, Akt3,* and *Frap1* through phosphorylation, compound action on the substrate, and indirect regulation [19]. On the other hand, its absence prevented the signaling transduction of PI3K/Akt. In contrast, *Ppp2r1a* acted as the negative regulator of signal pathways, including GnRH, MAPK/ERK, *etc.*, by inducing an inhibitory effect on various downstream proteins, such as *Prkca*, *Prkcc*, *Prkcb1*, *Map2k1*, *Map2k2*, and *Mapk3* [20].

The stepwise protein-protein interaction, ranging from 1 to 4 steps, led to alternations in the activity and/or expression of TFs (*Sp1, Jun, Crebl, Arnt, Fos, Nf1*), which thereby qualified them for the bottom layer of key nodes in the regulatory network. The signals of the MAPK/ERK and TGFβ/Smad signaling pathways were mapped to the TF binding domains of *Col1a1* (*Sp1*, *Nf1*), *Col3a1* (*Jun*), *Col5a3* (*Sp1*), *Col12a1* (*Sp1*), *Mmp*2 (*Jun*, *Fos*), *Cdc20* (*Sp1*)), *Cdkn1a* (*Sp1*, *Fos*), *Pttg1* (*Sp1*), *Wee1* (*Sp1*, *Fos*), *Birc3* (*Sp1*), *Casp3* (*Sp1*), *Ddit3* (*Jun*), *Dffa* (*Sp1*), and *Serpine1* (*Fos*). The signaling pathways of TGFβ/Smad and PI3K/Akt also controlled the *Casp9* expression level *via Arnt*. Furthermore, the PI3K/Akt signaling pathway modulated both *Mmp12* and *Tgfb2 via* the TF of *Crebl*. Consequently, the set of TFs was found to be an executor of the miR-16 regulatory network that bridged the gap between the targetome and transcriptome.

In conclusion, miR-16 exerts a wide-range effect on both the targetome and transcriptome of activated HSCs. A regulatory network of key targets and TFs underlies the signal transduction from the targetome to the transcriptome. Ultimately, integrating the targetome, transcriptome, and regulatory network uncovers the transcriptomic characteristics of miR-16-treated HSCs, including cell cycle arrest, collagen degradation, and apoptosis susceptibility. This global effect suggests that miR-16 plays an inhibitory role against the activation of HSCs.

Acknowledgement

References

[1] C.J. Guo, Q. Pan, B. Jiang, G.Y. Chen and D.G. Li, Effects of upregulated expression of microRNA-16 on biological properties of culture-activated hepatic stellate cells, Apoptosis **14** (2009), 1331–1340.

[2] L.P. Lim, N.C. Lau, P. Garrett-Engele, A. Grimson, J.M. Schelter, J. Castle, D.P. Bartel, P.S. Linsley and J.M. Johnson, Microarray analysis shows that some microRNAs downregulate large numbers of target mRNAs, Nature **433** (2005), 769–773.

[3] G.W. Wright and R.M. Simon, A random variance model for detection of differential gene expression in small microarray experiments, Bioinformatics **19** (2003), 2448–2455.

[4] S. Griffiths-Jones, R.J. Grocock, S. van Dongen, A. Bateman and A.J. Enright, miRBase: microRNA sequences, targets and gene nomenclature, Nucleic Acids Res. **34** (2006), D140–D144.

[5] B.P. Lewis, C.B. Burge and D.P. Bartel, Conserved seed pairing, often flanked by adenosines, indicates that thousands of human genes are microRNA targets, Cell **120** (2005), 15–20.

[6] G.D. Bader, I. Donaldson, C. Wolting, B.F. Ouellette, T. Pawson and C.W. Hogue, BIND-the biomolecular interaction network database, Nucleic Acids Research **29** (2001), 242–245.

[7] A. Chatr-Aryamontri, B.J. Breitkreutz, S. Heinicke, L. Boucher, A. Winter, C. Stark, J. Nixon, L. Ramage, N. Kolas, L. O'Donnell, T. Reguly, A. Breitkreutz, A. Sellam, D. Chen, C. Chang, J. Rust, M. Livstone, R. Oughtred, K. Dolinski and M. Tyers, The BioGRID interaction database: 2013 update, Nucleic Acids Research **41** (2013), D816–D823.

[8] M. Kanehisa, Molecular network analysis of diseases and drugs in KEGG, Methods in Molecular Biology **939** (2013), 263–275.

[9] T.M. Chan, K.C. Wong, K.H. Lee, M.H. Wong, C.K. Lau, S.K. Tsui and K.S. Leung, Discovering approximate-associated sequence patterns for protein-DNA interactions, Bioinformatics **27** (2011), 471–478.

[10] M. He, Q.Y. Wang, Q.Q. Yin, J. Tang, Y. Lu, C.X. Zhou, C.W. Duan, D.L. Hong, T. Tanaka, G.Q. Chen and Q. Zhao, HIF-1α downregulates miR-17/20a directly targeting p21 and STAT3: a role in myeloid leukemic cell differentiation, Cell Death Differ. **20** (2013), 408–418.

[11] M. Yi, J.D. Horton, J.C. Cohen, H.H. Hobbs and R.M. Stephens, Whole Pathway Scope: a comprehensive pathway-based analysis tool for high-throughput data, BMC Bioinformatics **7** (2006), 30–53.

[12] J. Jiang, X. Yuan, H. Zhao, X. Yan, X. Sun and Q. Zheng, Licochalcone A inhibiting proliferation of bladder cancer T24 cells by inducing reactive oxygen species production, Bio-Medical Materials and Engineering **24** (2014), 1019–1025.

[13] L.D. Hernández-Ortega, B.E. Alcántar-Díaz, L.A. Ruiz-Corro, A. Sandoval-Rodriguez, M. Bueno-Topete, J. Armendar-iz-Borunda and A.M. Salazar-Montes, Quercetin improves hepatic fibrosis reducing hepatic stellate cells and regulating pro-fibrogenic/anti-fibrogenic molecules balance, Journal of Gastroenterology and Hepatology **27** (2012), 1865–1872.

[14] Y.B. Ji, C.F. Ji and L. Yue, Human gastric cancer cell line SGC-7901 apoptosis induced by SFPS-B2 via a mitochon-drial-mediated pathway, Bio-Medical Materials and Engineering **24** (2014), 1141–1147.

[15] R.L. Kortum, A.K. Rouquette-Jazdanian and L.E. Samelson, Ras and extracellular signal-regulated kinase signaling in thymocytes and T cells, Trends in Immunology **34** (2013), 259–268.

[16] N. Maeda, N. Kawada, S. Seki, T. Arakawa, K. Ikeda, H. Iwao, H. Okuyama, J. Hirabayashi, K. Kasai and K. Yoshiza-to, Stimulation of proliferation of rat hepatic stellate cells by galectin-1 and galectin-3 through different intracellular signaling pathways, Journal of Biological Chemistry **278** (2003), 18938–18944.

[17] A. Hauburger, S. von. Einem, G.K. Schwaerzer, A. Buttstedt, M. Zebisch, M. Schräml, P. Hortschansky, P. Knaus and E. Schwarz, The pro-form of BMP-2 interferes with BMP-2 signalling by competing with BMP-2 for IA receptor bind-ing, FEBS Journal **276** (2009), 6386–6398.

[18] Q. Liu, X. Wang, Y. Zhang, C.J. Li, L.H. Hu and X. Shen, Leukamenin F suppresses liver fibrogenesis by inhibiting both hepatic stellate cell proliferation and extracellular matrix production, Acta. Pharmacologica. Sinica. **31** (2010), 839–848.

[19] G. Wang, C. Chen, R. Yang, X. Cao, S. Lai, X. Luo, Y. Feng, X. Xia, J. Gong and J. Hu, p55PIK-PI3K stimulates angi-ogenesis in colorectal cancer cell by activating NF-κB pathway, Angiogenesis **16** (2013), 561–573.

[20] P. Ramanathan, I.C. Martin, M. Gardiner-Garden, P.C. Thomson, R.M. Taylor, C.J. Ormandy, C. Moran and P. Wil-liamson, Transcriptome analysis identifies pathways associated with enhanced maternal performance in QSi5 mice, BMC Genomics **9** (2008), 197–209.